Energy Transfer in Ion–Molecule Collisions. Collisional Deactivation of $(C_5H_9^+)^*$

P. G. Miasek and A. G. Harrison*[1]

Contribution from the Department of Chemistry, University of Toronto, Toronto, Canada M5S 1A1. *Received March 18, 1974*

Abstract: The relative rates of formation of $C_5H_9^+$ and $C_5H_7^+$ by reaction of $C_3H_5^+$ with ethylene have been studied both in pure ethylene and in mixtures of ethylene with various bath gases M. From the variation of the ratio $[C_5H_9^+]/[C_5H_7^+]$ with pressure of the bath gas, relative collisional stabilization efficiencies of $(C_5H_9^+)^*$ by the various monatomic, diatomic, triatomic, and polyatomic bath gases have been determined. The relative stabilization efficiencies are not consistent with a mechanism where the efficiency of energy transfer is determined by the collision duration, approximated by the ion fly-by time. Rather the results indicate formation of a long-lived complex similar to that postulated by Rabinovitch for neutral–neutral systems. In this model deactivation results from energy redistribution involving the transitional modes of the complex with only minor involvement of the internal vibrational modes of the bath gas.

Energy transfer on collision between vibrationally excited molecules and ground state molecules has been the subject of considerable theoretical and experimental investigation. For diatomics in the low-energy region (one vibrational quantum), theory predicts[2-4] that energy transfer is most efficient for "hard" collisions, with a steep repulsive potential energy well, where the collision duration is thus comparable to the vibration period. Transition probabilities ($v = 1$ to 0) are predicted to range from 10^{-3} to 10^{-9} per collision and to increase with increasing temperature. This is in reasonable agreement with much of the experimental data.[5,6] For species (both diatomic and more complex) with considerably higher vibrational excitation, different results are obtained experimentally in that it frequently is observed[7-11] that the efficiency of energy transfer (vibrational → translational) on collision increases with increasing collision duration reaching a maximum when the vibrational frequency matches the "frequency" of the collision duration. Detailed theoretical treatments are not yet available.

Extensive studies of the collisional deactivation of highly vibrationally excited molecules, such as those arising during chemical reactions, have been carried out by Rabinovitch and coworkers.[12-17] These results have been incorporated[16] into a model of vibrational deactivation, based on the RRKM theory, which assumes that the activated molecule (termed the substrate) and the (inert) bath gas form a complex in which energy redistribution occurs among the internal modes of the substrate and the transitional modes of the complex; the transitional modes are vibrational modes of the complex correlating with relative translational and rotational motion of the colliding partners. Unrestricted energy redistribution is not permitted as the allowed energy in bending modes of the complex is limited by angular momentum conservation requirements. Implicit in the subsequent experimental analysis is the usual Lindemann assumption that only one collision is sufficient for deactivation. This has been confirmed experimentally. The experimental results are in general agreement with the above model and demonstrate that vibrational energy of the substrate is converted primarily to translational and rotational energy of the colliding partners. Three classes of bath gases can be distinguished, monatomic, linear and diatomic, and polyatomic, according to the number of transitional modes available in the complex. Equilibration involving internal vibrational modes of the bath gas appears to be significant only for very efficient deactivators and, even in these cases, represents only a minor contribution to the total collisional deactivation efficiency.

Further aspects[18,19] of Rabinovitch's work, using chemically activated molecules, have involved the study of multistep deactivation processes to determine probability distributions for ΔE, the energy lost from the substrate per collision. These studies have shown[20] that inefficient collision gases do not have a large number of elastic collisions and a few efficient ones, but rather that most collisions remove some energy, the average amount removed per collision being small. Thus, variations in the efficiencies of the single-collision stabilization process of Lindemann theory must be interpreted in terms of variations in the fraction of collisions that remove an energy ΔE which is equal to or greater than that necessary for deactivation. This should hold also for the ion–molecule collisions investigated in this work.

In contrast to the rather extensive studies in neutral systems there have been very few studies of collisonal energy transfer processes for vibrationally excited ions. In the low-energy region Shin[21] has used the method of Zener[2] to predict that the strong ion–neutral attractive interaction should result in a "harder" (or shorter duration) collision and thus increase the probability of energy transfer. In the high-energy region there have been no extensive systematic studies similar to the neutral studies of Rabinovitch involving a wide variety of collision gases with differing properties. Such studies would have the distinct advantage that the collision rate for nonpolar bath gases can be estimated accurately from the Langevin ion-induced dipole collision model.[22]

To our knowledge there have been only two systematic investigations of energy transfer in gaseous ionic systems.[23] Gill, Inel, and Meisels[26] have studied the collisional deactivation of $(C_4H_8^+)^*$ by various inert gases in the radiolysis of ethylene. They invoked a *series* of successive deactivating collisions with the third body to reduce the internal energy and interpreted the observed product distributions in this light. They concluded that energy transfer in nonreactive ion–molecule collisions is considerably less that anticipated on the basis of formation of an intermediate complex where all the internal degrees of freedom are active.

Very recently Anicich and Bowers[27] have measured absolute third-order rate coefficients for formation of the dimers $(CH_2CF_2^+{\cdot}CH_2CF_2)$ and $(C_6H_6^+{\cdot}C_6H_6)$ in mixtures of the respective parent gases, CH_2CF_2 or C_6H_6, with nonreactive bath gases. From these rate coefficients they estimated relative stabilization efficiencies per collision for the rare gases, N_2, CO, and the parent gases. Except for C_6H_6 stabilization of $(C_6H_6^+{\cdot}C_6H_6)$ they observed a linear dependence of the collision efficiency on $\mu^{1/2}$ (μ = reduced mass of colliding pair), which they interpreted as indicating vibrational-translational energy transfer with the probability depending on the collision duration.

As an initial study of energy transfer in ionic systems we have chosen to study the collisional deactivation of the excited ion $(C_5H_9^+)^*$ produced in ethylene. The ionic chemistry of ethylene has been studied extensively[28-31] and there is general agreement as to the reactions occurring. The relevant reaction sequence for this work is that initiated by the molecular ion, as summarized in Scheme I. Other minor ions, notably $C_3H_4^+$, form less than 2% of the total product yield[31] from reaction of $C_2H_4^+$ and will be neglected in this study. The secondary ion $C_4H_7^+$ is formed in about 8% yield and does not appear to react further.[31]

Scheme I

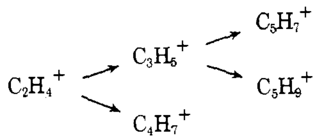

The detailed mechanism for formation of $C_5H_7^+$ and $C_5H_9^+$ is apparently quite complicated. Both ions result from reaction of $C_3H_5^+$ with C_2H_4 to form an excited species, $(C_5H_9^+)^*$, which can either decompose back to reactants,[29,32] decompose to $C_5H_7^+ + H_2$, or be collisionally deactivated to form stable $C_5H_9^+$.[29,32] The observation[29] that, in the reaction of $C_3H_5^+$ with C_2D_4 in a tandem mass spectrometer, there is considerable production of $C_3(H,D)_5^+$ ions indicates the formation of a relatively long-lived collision complex. The simplest mechanism[30] to describe the formation of $C_5H_7^+$ and $C_5H_9^+$, and the one we will employ in this work, is outlined in Scheme II, where M is any third body. This mechanism differs from most simple termolecular schemes[24,25] by including both a unimolecular and a collision-induced route for formation of the $C_5H_7^+$ product. Both are necessary to rationalize the pressure dependence of the ion abundances in ethylene, although other, still more complex, mechanisms can also be invoked and lead to essentially the same predictions as Scheme II in the low-pressure region.

Scheme II

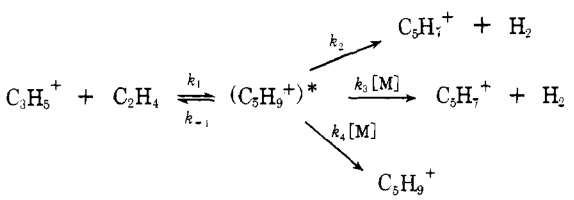

From Scheme II we may derive the kinetic expression in (1) for R, the observed ratio $[C_5H_9^+]/[C_5H_7^+]$, in mixtures of ethylene with a second gas M. Equation 1 predicts that, in pure ethylene, R should initially increase linearly with $[C_2H_4]$ ($k_3[C_2H_4] \ll k_2$) with a slope k_4/k_2.[33] In mixtures of ethylene with an inert third body at constant (low) values of $[C_2H_4]$, R should initially increase linearly with [M] with a limiting slope given by k_4'/k_2. The present work involved the determination of the ratio k_4'/K_2 for a variety of bath gases, and, thus, the determination of relative collisional stabilization efficiencies. (Note that the collision-induced decomposition processes (k_3 and k_3') are unimportant when initial slopes are employed.) The experimental results are compared with similar results for neutral systems obtained by Rabinovitch et al. and are compared with theories developed for neutral systems.

$$R = \frac{[C_5H_9^+]}{[C_5H_7^+]} = \frac{k_4[C_2H_4]}{k_2 + k_3[C_2H_4] + k_3'[M]} + \frac{k_4'[M]}{k_2 + k_3[C_2H_4] + k_3'[M]} \quad (1)$$

Experimental Section

The experimental work was carried out using the mass spectrometer and ion-trapping techniques described previously.[31] In this technique, ions are produced during a short (5 μsec) pulse of electrons of suitable energy and are trapped in the negative space charge of a continuous electron beam of energy insufficient to cause ionization. A positive voltage pulse applied to the repeller electrode a known and variable time after the ionizing pulse removes the ions for mass analysis in a conventional magnetic deflection mass spectrometer. Delay times between the ionizing and withdrawal pulses (and, hence, reaction times) of up to 4 msec may be used. In the present work two types of studies were made. In pure ethylene and in mixtures with various third bodies, the ion intensities were observed as a function of reaction time at constant source pressures to determine the products of reaction and the relevant rate constants. In addition, runs were carried out at a constant reaction time (usually 1.0 msec) by varying the pressure of ethylene or added third body to permit measurement of relative collisional stabilization rate constants by use of eq 1.

Source concentrations were not measured directly but were related to the gas pressures in each of two sample inlet systems. Tests showed that the source concentration was a linear function of the sample pressure in either inlet system and was independent of the identity of the gas. Two-component mixtures in the ion source were obtained by using known pressures of the two gases separately in the two inlet systems. For each inlet system the relation between source concentration and inlet pressure was established by observation of the $CH_4^+ + CH_4$ reaction in pure methane; all rate coefficients are therefore relative to the value[34] of 1.20×10^{-9} cm^3 molecule^{-1} sec^{-1} for this reaction. In all experiments the source temperature was approximately 100°.

All unlabeled compounds were commercially available and showed no detectable impurities in their mass spectra. Methane-d_4 and ethane-d_6 were obtained from Merck Sharp and Dohme, Montreal.

The average kinetic energy of primary ions in the ion trap has previously been determined[31] to be approximately 0.4 eV. This kinetic energy is related to the ion-trap potential well depth, which is predicted[35] to be proportional to $I_e/E_e^{1/2}$, where I_e is the electron current and E_e is the electron energy. It was not possible to verify this dependence experimentally as trapping efficiencies rapidly deteriorated as I_e and E_e were altered from their optimum values. The day-to-day fluctuations in the optimum value of I_e were not great (±20%) and are thus expected to have little effect on the rates of processes that are relatively insensitive to ion kinetic energy. However, the lifetime of the $(C_5H_9^+)^*$ collision complex may be quite sensitive to ion kinetic energy and variation of this energy may be the cause of some of the experimental scatter observed, particularly for absolute termolecular rate constants.

Results and Discussion

A. Pure Ethylene. The rather complex mechanism of Scheme II is cumbersome for kinetic analysis and, for pure ethylene, its main features can be represented by reactions 2-4. From a steady-state analysis on $(C_5H_9^+)^*$ (Scheme II)

$$C_3H_5^+ + 2C_2H_4 \xrightarrow{k_a} C_5H_9^+ + C_2H_4 \quad (2)$$

$$C_3H_5^+ + C_2H_4 \xrightarrow{k_b} C_5H_7^+ + H_2 \quad (3)$$

$$C_3H_5^+ + 2C_2H_4 \xrightarrow{k_c} C_5H_7^+ + (H_2 + C_2H_4) \quad (4)$$

we may derive the following relationships between the overall rate coefficients, k_a, k_b, and K_c, and those used in Scheme II.

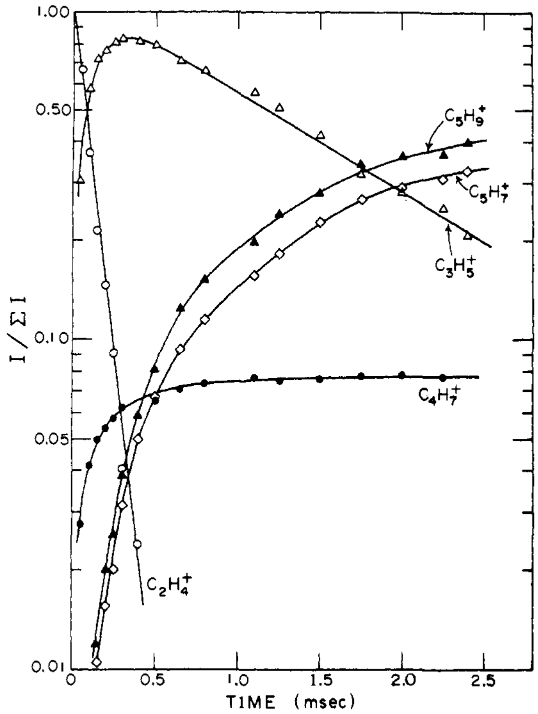

Figure 1. Time dependence of ionic abundances in ethylene, low electron energy. $[C_2H_4] = 1.15 \times 10^{13}$ molecules cm^{-3}.

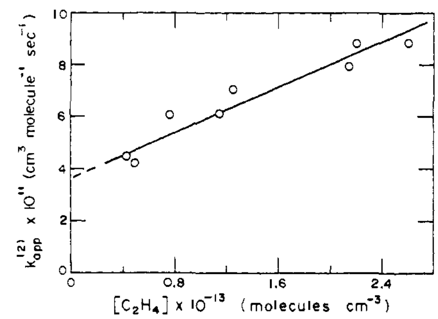

Figure 2. Determination of absolute bimolecular and termolecular rate constants for reaction of $C_3H_5^+$ in pure ethylene (see text). The straight line represents a least-squares fit of the experimental points.

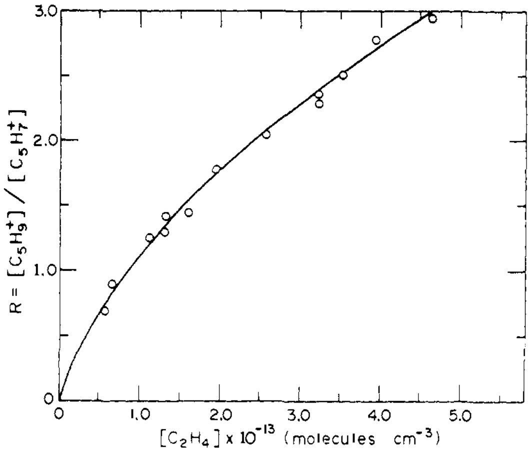

Figure 3. Concentration dependence of $R = [C_5H_9^+]/[C_5H_7^+]$ in pure ethylene. Reaction time = 1.0 msec.

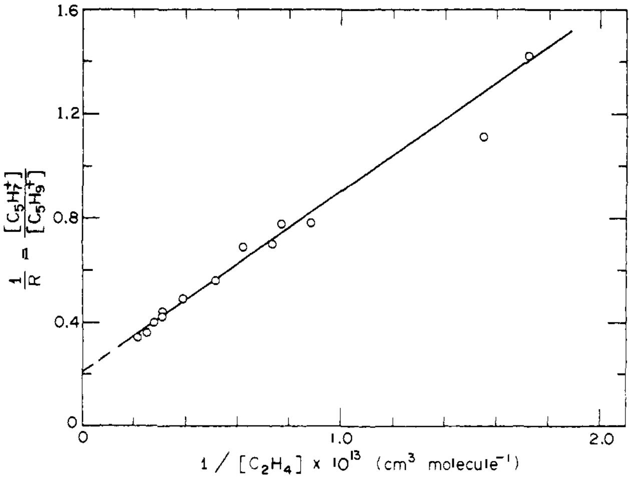

Figure 4. Variation of $1/R$ with $1/[C_2H_4]$ in pure ethylene, data from Figure 3. The straight line is a least-squares fit of all experimental data except two points at low pressures (high $1/[C_2H_4]$) which are subject to large error. Inclusion of these two points changes intercept and slope by less than 10%.

$$k_a = \frac{k_1k_4}{k_{-1} + k_2 + k_3[C_2H_4] + k_4[C_2H_4]} \approx \frac{k_1k_4}{k_{-1}} \quad (5)$$

$$k_b = \frac{k_1k_2}{k_{-1} + k_2 + k_3[C_2H_4] + k_4[C_2H_4]} \approx \frac{k_1k_2}{k_{-1}} \quad (6)$$

$$k_c = \frac{k_1k_3}{k_{-1} + k_2 + k_3[C_2H_4] + k_4[C_2H_4]} \approx \frac{k_1k_3}{k_{-1}} \quad (7)$$

The approximate relationships will be shown below to be valid for the low-pressure conditions ($<10^{-3}$ Torr) employed in this work.

For the overall reactions 2-4 we may derive the following expression for the disappearance of $C_3H_5^+$ at reaction times greater than that necessary for complete reaction of $C_2H_4^+$.

$$2.303 \log [C_3H_5^+] = -(k_a[C_2H_4]^2 + k_b[C_2H_4] + k_c[C_2H_4]^2)t + \text{constant} \quad (8)$$

It is convenient to define an apparent bimolecular rate coefficient, $k_{app}^{(2)}$, for disappearance of $C_3H_5^+$, which is related to the slope of the plot of log $[C_3H_5^+]$ *vs.* t at constant C_2H_4 concentration by

$$k_{app}^{(2)} = 2.303 \text{ slope}/[C_2H_4] \quad (9)$$

and is related to the rate coefficients of eq 8 in eq 10. A plot of $k_{app}^{(2)}$ *vs.* $[C_2H_4]$ should yield a straight line of slope $k_a + k_c$ and intercept k_b.

$$k_{app}^{(2)} = (k_a + k_c)[C_2H_4] + k_b \quad (10)$$

In addition, the ratio $[C_5H_9^+]/[C_5H_7^+]$ is given by

$$R = \frac{[C_5H_9^+]}{[C_5H_7^+]} = \frac{k_a[C_2H_4]}{k_b + k_c[C_2H_4]} \quad (11)$$

and a plot of R *vs.* $[C_2H_4]$ should have a maximum limiting slope at low $[C_2H_4]$ of $k_a/k_b = K_4/k_2$ ($k_c[C_2H_4] \ll k_b$). Alternatively, a plot of $1/R$ *vs.* $1/[C_2H_4]$ should be a straight line with a slope K_b/k_a ($=k_2/k_4$) and an intercept k_c/k_a ($=k_3/k_4$).

Typical experimental results for pure ethylene are shown in Figures 1-4. Figure 1 is a standard ion abundance (logarithmic scale) *vs.* reaction time plot and is our typical experimental data. Only the five ion intensities shown were monitored. At high pressures and long reaction times a maximum of 3% of higher order products ($C_6H_n^+$, $C_7H_n^+$) was observed; these were not investigated further. The rate coefficient $k_{app}^{(2)}$ is determined directly from the slope of the $C_3H_5^+$ disappearance curve at times where its formation from $C_2H_4^+$ is negligible. Figure 2 shows a plot of $k_{app}^{(2)}$ *vs.* $[C_2H_4]$ (eq 10). A least-squares analysis gives k_a

$+ k_c = 2.2 \pm 0.5 \times 10^{-24}$ cm^6 molecule^{-2} sec^{-1} and $k_b = 3.7 \pm 0.7 \times 10^{-11}$ cm^3 molecule^{-1} sec^{-1}. The scatter in the data may arise, in part, from small day-to-day changes in the optimum ion trapping conditions (see Experimental Section). The magnitudes of the rate coefficients depend critically on the lifetime $(1/(k_{-1} + k_2))$ of $(C_5H_9^+)^*$ which is determined, in part, by the internal energy of the species, which in turn depends on the kinetic energy of the $C_3H_5^+$ precursor.

Figure 3 shows a plot of R *vs.* $[C_2H_4]$ (eq 11) at constant reaction time (1 msec). As predicted, this is not linear but shows a decreasing slope with increasing $[C_2H_4]$ due to the influence of the $k_c[C_2H_4]$ term in the denominator of eq 11. From the initial slope we obtain $k_a/k_b = 1.3 \pm 0.2 \times 10^{-13}$ cm^3 molecule^{-1}. In terms of Scheme II this ratio equals k_4/k_2. Figure 4 shows a plot of $1/R$ *vs.* $1/[C_2H_4]$ for the same data. This yields a linear plot from which we derive from the slope $k_a/k_b = 1.4 \times 10^{-13}$ cm^3 molecule^{-1}, and from the intercept k_a/k_c $(=k_4/k_3) \approx 5$. This latter value is in good agreement with the value of ~6.5 estimated by Bowers, *et al.*,[30] from an analysis of the experimental data of Myher and Harrison.[28] The value $k_a/k_b = 1.4 \times 10^{-13}$ cm^3 molecule^{-1} is very close to the value of 1.3×10^{-13} cm^3 molecule^{-1} derived from the initial slope of Figure 3, but is considerably higher than the value of $\sim 4.7 \times 10^{-14}$ cm^3 molecule^{-1} which may be derived from the slope and intercept of Figure 2 (assuming $k_c = 0.2k_a$). The uncertainty in the latter value for k_a/k_b is large, however. We thus conclude that the following approximate rate coefficients are appropriate for the ethylene system under our experimental conditions: $k_a \approx 3 \times 10^{-24}$ cm^6 molecule^{-2} sec^{-1}; $k_b \approx 3 \times 10^{-11}$ cm^3 molecule^{-1} sec^{-1}; $k_c \approx 6 \times 10^{-25}$ cm^6 molecule^{-2} sec^{-1}. The present value of k_a is somewhat higher than the values of 0.4 to 1.4×10^{-24} cm^6 molecule^{-2} sec^{-1} reported by Harrison and Herod.[32] This may result from differences in the ion kinetic energy distributions in the two experiments.[36]

Assuming a steady state in $(C_5H_9^+)^*$, eq 12 represents $k_{app}^{(2)}$ in terms of the rate coefficients in Scheme II. If k_1,

$$k_{app}^{(2)} = k_1\left(\frac{k_2 + k_3[C_2H_4] + k_4[C_2H_4]}{k_{-1} + k_2 + k_3[C_2H_4] + k_4[C_2H_4]}\right) \quad (12)$$

the rate coefficient for reactive collision between $C_3H_5^+$ and C_2H_4, is assumed to be comparable to the Langevin collision rate, we observe from Figure 2 that $k_{app}^{(2)}$ is only 3-8% of k_1. This low value must imply that $k_{-1} \gg k_2 + k_3[C_2H_4] + k_4[C_2H_4]$ at the source concentrations employed in the present work. Thus the approximations used in eq 5-7 are justified.

B. Mixtures of Ethylene with a Second Bath Gas. Addition of an inert bath gas to the ethylene system introduces an additional reaction resulting in collisional stabilization of $(C_5H_9^+)^*$, as well as an additional reaction leading to collision-induced dissociation to $C_5H_7^+ + H_2$. The system becomes extremely complex for a complete kinetic analysis; however, in the present work we are most interested in the collisional stabilization process. For Scheme II the ratio R is given by eq 1. We have shown above that at low ethylene concentrations $k_3[C_2H_4] \ll k_2$. Thus at constant low ethylene concentration the plot of R *vs.* [M] should have an initial slope given by k_4'/k_2 (*i.e.*, $k_3'[M] \ll k_2$).

We have thus obtained relative values of k_4'/k_2 from the initial slopes of such plots for various bath gases M. Typical results are shown in Figure 5 for a reaction time of 1.0 msec, greater than that necessary for reaction of primary $C_2H_4^+$. Approximately the same ethylene concentration ($\sim 6 \times 10^{12}$ molecules cm^{-3}) was used in each run and the electron energy was maintained below the ionization potential of the bath gas. No products of ion-molecule reactions involving M were detected except for the C_2H_6 and C_2D_6 systems which will be discussed in greater detail below.

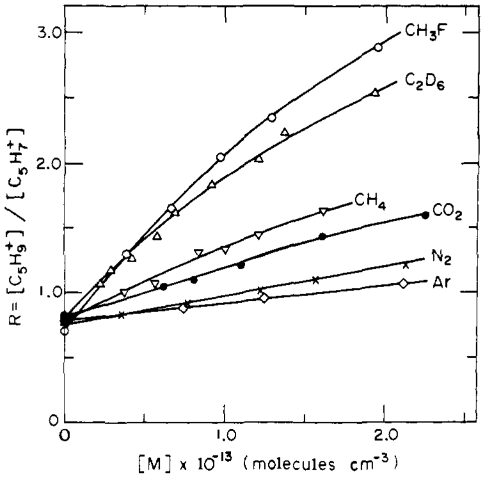

Figure 5. Variation of $R = [C_5H_9^+]/[C_5H_7^+]$ with concentration of collision gas M. $[C_2H_4] \approx 6 \times 10^{12}$ molecules cm^{-3}. Reaction time = 1.0 *m*sec.

The plots of R *vs.* [M] show initial linear regions followed by downward curvature at higher values of [M] as the slower collision-induced decomposition to $C_5H_7^+$ ($k_3'[M]$) becomes a significant contributor to the total $C_5H_7^+$ yield. However, reasonably accurate values of k_4'/k_2 may be determined from the initial slopes. The changes in the initial slopes as the bath gas is changed are assumed to be due to variations in k_4', the collisional stabilization rate coefficient. These are reported in Table I as k_a' relative to the value of $k_a(k_4/k_2)$ obtained from the similar plot in pure ethylene (Figure 3). The numbers in Table I, column 2, thus represent relative collisional stabilization rate coefficients for the various gases M. The absolute value of the termolecular rate coefficient, k_a', for the process

$$C_3H_5^+ + C_2H_4 + M \xrightarrow{k_a'} C_5H_9^+ + M \quad (13)$$

can be obtained for any M from the absolute value of k_a for pure ethylene reported above.

C. Ion-Molecule Reactions in C_2H_4-C_2H_6 Mixtures. As mentioned previously, side reactions were observed in this study in ethylene-ethane mixtures. A detailed analysis of these reactions is beyond the scope of this paper; however, it is important to ascertain if there are any additional reactions leading to $C_5H_7^+$ or $C_5H_9^+$. Such reactions, if of sufficient importance, could obscure any inferences derived from a plot of R *vs.* $[C_2H_6]$ concerning collisional stabilization by C_2H_6.

In a 2:1 mixture of C_2H_6 and C_2H_4 (total source concentration = 1.4×10^{13} molecules cm^{-3}), at an electron energy nominally below the ionization potential of C_2H_6, approximately 2% $C_2H_6^+$ was observed at short trapping times while about 2% $C_3H_7^+$ was observed at 1 msec. trapping time. No other products not observed in pure ethylene were detected. In a similar C_2D_6-C_2H_4 mixture under the same conditions, a considerable variety of additional product ions was observed, as reported in Table II. The ions of *m/e* 71 to 73 are of greatest interest since they may represent $C_5(H,D)_7^+$ or $C_5(H,D,)_9^+$ ions formed by a route additional to that given in Scheme II. However, for the sake of completeness we list in the Appendix the other reactions that appear to occur in this system. These reactions do not interfere with the collisional stabilization studies of this paper.

Ions of *m/e* 71-73 probably arise from reactions 14 to 16, although it is possible that *m/e* 73 could be $C_5H_5D_4^+$. Thus

Table I. Relative Collisional Stabilization Rate Coefficients and Efficiencies[a]

M	k_a'	k_a'/k_{LANG}	k_a'/k_{LD}, eV 0.4	0.3	0.2	Thermal	Best value
C_2H_4	(1.00)	(1.00)					(1.00)
He	0.097	0.19					0.19
Ne	0.073	0.21					0.21
Ar	0.127	0.235					0.235
Kr	0.103	0.19					0.19
H_2	0.23	0.165					0.165
D_2	0.22	0.22					0.22
N_2	0.205	0.325					0.325
CO_2	0.365	0.53					0.53
CH_4	0.54	0.57					0.57
CD_4	0.51	0.58					0.58
CF_4	0.44	0.76					0.76
SF_6	0.545	0.83					0.83
C_2H_6	1.02	1.02					1.02
C_2D_6	0.90	0.98					0.98
CO	0.255	0.38	0.34	0.33	0.33	0.30	0.33
N_2O	0.44	0.62	0.54	0.53	0.52	0.30	0.53
SO_2	0.96	1.33	0.65	0.60	0.54	0.31	0.62
CH_3F	1.16	1.61	0.59	0.54	0.48	0.30	0.57
CH_2F_2	1.26	1.96	0.75	0.68	0.61	0.35	0.71
CF_2Cl_2	0.60	0.74	0.60	0.58	0.56	0.41	0.59

[a] See text for discussion of calculation of relative stabilization efficiencies.

Table II. Peaks Observed in a 2:1 C_2D_6–C_2H_4 Mixture[a,b]

Mass range	Identification	% total ioniz	Remarks
32	$C_2D_4^+$	3	Short trapping times
36	$C_2D_6^+$	2	Short trapping times
42–44	$C_3H_4D^+$, $C_3H_3D_2^+$, $C_3H_2D_3^+$	8	Long trapping times
46–49	$C_3H_4D_3^+$, $C_3H_3D_4^+$, $C_3H_2D_5^+$, $C_3HD_6^+$	2	Long trapping times
58, 59	$C_4H_4D_3^+$, $C_4H_3D_4^+$	0.3	Long trapping times
71–73	See text	0.4	Long trapping times

[a] Experimental conditions given in text. [b] Peaks observed in pure C_2H_4 are not reported.

$$C_3H_5^+ + C_2D_6 \longrightarrow C_5HD_6^+ + 2H_2 \qquad m/e\ 73 \quad (14)$$

$$C_3H_5^+ + C_2D_6 \longrightarrow C_5H_2D_5^+ + HD + H_2 \qquad m/e\ 72 \quad (15)$$

$$C_3H_5^+ + C_2D_6 \longrightarrow C_5H_3D_4^+ + 2(H,D)_2 \qquad m/e\ 71 \quad (16)$$

formation of $C_5H_7^+$ (and, possibly, $C_5H_9^+$) by reaction of $C_3H_5^+$ with C_2H_6 does occur. The extent of these reactions is sufficiently small (*m/e* 71–73 intensities about 5% of total $C_5H_7^+ + C_5H_9^+$ intensities) that a negligible influence will be exerted on *R* and thus on the relative collisional stabilization rate coefficient derived for C_2H_6. This conclusion is supported by the good agreement of the results for C_2H_6 and C_2D_6.

D. Relative Stabilization Efficiencies. The experimental data recorded in column 2 of Table I represent relative collisional stabilization rate coefficients. For meaningful comparisons these rate coefficients must be normalized by dividing by the relative collision rate constants to obtain relative stabilization efficiencies *per collision.* For nonpolar bath gases the collision rate constant was calculated from the Langevin model,[22] *i.e.*

$$k_{LANG} = 2\pi e(\alpha/\mu)^{1/2} \qquad (17)$$

where α is the angle-averaged polarizability of the neutral, *e* is the electronic charge, and μ is the reduced mass of the colliding pair. The relative stabilization efficiencies so calculated are given in column 3. This approach assumes that the rate of collision is determined by ion-induced dipole interactions. For polar bath molecules there is an additional ion–dipole interaction and there are no simple formulations that yield exact expressions for the collision rate constant. Accordingly three different approaches have been used. The first of these neglects the effect of ion–dipole interactions and employs eq 17 to calculate collision rate coefficients. These represent lower limits to the collision rate coefficients and, correspondingly, the relative stabilization efficiencies for polar molecules listed in column 3 of Table I represent upper limits.

Theoretical treatments that include the effect of ion–dipole interactions frequently employ the "locked-dipole" model where the dipole is assumed to remain aligned with the charged ion throughout the collision. This model results in the following expression[37] for the collision rate coefficient

$$k_{LD} = 2\pi e\left(\frac{\alpha}{\mu}\right)^{1/2} + \frac{2\pi ep}{(2E\mu)^{1/2}} \qquad (18)$$

where *E* is the relative kinetic energy of the colliding pair and *p* is the dipole moment of the polar neutral species. The upper limit to the collision rate coefficient occurs at thermal energies where eq 18 becomes[34]

$$k_{LD} = 2\pi e\left(\frac{\alpha}{\mu}\right)^{1/2} + 2\pi ep\left(\frac{2\mu}{kT}\right)^{1/2} \qquad (19)$$

where *T* is the temperature and *k* is Boltzmann's constant. This represents an upper limit to the collision rate coefficient and, hence, the relative stabilization efficiencies listed in column 7 of Table I for polar molecules represent lower limits.

Undoubtedly the actual situation is somewhere between the two extremes represented by eq 17 and 19. It has been observed[38,39] that rate constants for highly exothermic proton transfer reactions to polar molecules (expected to have nearly unit collisional efficiency) measured by the trapped ion technique generally are in good agreement with collision rate coefficients calculated by eq 18 using an ion kinetic energy (laboratory scale) of 0.2 to 0.4 eV and thermal kinetic energies for the neutral molecule. While this result has no theoretical significance, it does suggest that, in the present work, collision rate coefficients for polar bath gases can be estimated in the same manner. The resulting relative stabilization efficiencies are listed in columns 4 to 6 of Table I for each of the assumed ion kinetic energies 0.4, 0.3, and 0.2 eV.

Assuming that the differences in stabilization efficiencies in the series CH_4 (p = 0), CH_3F (p = 1.9 D), CH_2F_2 (p =

1.9 D), and CF_4 ($p = 0$) follow a systematic trend, it can be seen from Table I that the thermal "locked-dipole" expression overestimates the effect of ion–dipole interactions while neglect of ion–dipole interactions by using the Langevin expression also is unable to reproduce the expected trend. On the other hand using the "locked-dipole" expression (eq 18) at an ion kinetic energy of 0.3–0.4 eV to calculate the collision rate coefficients results in relative stabilization efficiencies which adequately reproduce the expected trend. Further, one might expect the three triatomic bath gases CO_2, N_2O, and SO_2 to have similar stabilization efficiencies and this is found only if the collision rate coefficients for the polar gases N_2O and SO_2 are calculated assuming ion kinetic energies of 0.3–0.4 eV. Thus we conclude that, for ion–polar molecule collisions in the trapped ion technique, the effect of ion–dipole interactions on the collision rate can be approximated reasonably accurately using eq 18 at an ion kinetic energy of 0.3–0.4 eV. The present results are therefore in agreement with previous results[38,39] for reactions involving other than primary ions.[40]

The final column in Table I presents our "best" values for the relative stabilization efficiencies per collision for the bath gases used. These numbers will be employed in the remainder of the discussion.

E. Comparison with Previous Results and Theories. 1. Ionic Systems. In view of the results of Shin[21] concerning the effect of the strong ion–neutral interaction on the "hardness" of the collision, and thus the efficiency of energy transfer, an investigation of the dependence of the stabilization efficiency on $-(\partial V/\partial r)$, the steepness of the repulsive wall, is of interest. For a nonpolar molecule the potential energy is given by

$$V(r) = \frac{-e^2\alpha}{2r^4} + 4\epsilon\left[\left(\frac{\sigma}{r}\right)^{12} - \left(\frac{\sigma}{r}\right)^{6}\right] \quad (20)$$

where α is the molecular polarizability and ϵ and σ are the Lennard-Jones coefficients for the colliding pair. The values of ϵ and σ and the combining rules listed in ref 13 were used. For $C_5H_9^+$ ϵ was taken as 4.3×10^{-14} erg and σ as 5.65 Å, comparable to the coefficients appropriate for C_5H_{10} or C_5H_8. The derivative was evaluated at $V(r) = 0$, corresponding to a collision with near-thermal kinetic energy, and at $V(r) = 0.4$ eV and $0.4\ \mu/m_i$ eV (m_i = ion mass), corresponding to nonthermal kinetic energies. No correlation of the stabilization efficiencies with $-(\partial V/\partial r)$ was found at any of these energies, in agreement with the findings of Rabinovitch, *et al.*,[13] for neutral systems. Our results for $V(r) = 0$ are shown in Figure 6 for illustrative purposes.

The dependence of the stabilization efficiency on polarizability, dipole moment, and boiling point was also investigated. The estimation of the collision rates in polar systems has adequately accounted for the effect of the dipole moment and hence no correlation with dipole moment exists. A general trend of increasing stabilization efficiency with increasing polarizability or increasing boiling point was noted. As will be shown below, this is primarily a result of the dependence of the stabilization efficiency on molecular complexity.

Qualitative inferences concerning relative collisional stabilization efficiencies of simple gases have been obtained from the study of termolecular ion–molecule reactions. In these studies[24,25] the relative order He < Ar < N_2 has invariably been found. Our results are in agreement.

The most extensive study comparable to this work has been the recent study by Anicich and Bowers[27] of the collisional stabilization of $(CH_2CF_2{\cdot}CH_2CF_2^+)^*$ and $(C_6H_6{\cdot}C_6H_6^+)^*$ by the rare gases, N_2, and CO. They found that the stabilization efficiencies increased linearly with the square root of the reduced mass of the colliding pair. This was taken as evidence that the probability of energy transfer depended on the duration of the collision, defined by the ion–neutral fly-by time which is proportional to the relative velocity (and, hence, $\mu^{1/2}$). Despite a 20-fold change in mass, our data exhibit little change in stabilization efficiencies for the rare gases, while N_2 and CO have stabilization efficiencies which are considerably higher. Thus the model used by Anicich and Bowers does not appear to be applicable to our system. The collision duration model implies that a long-lived complex (*i.e.*, with a lifetime considerably longer than the fly-by time) is not formed. The lack of agreement of our results with this model suggests the possibility that a long-lived complex may be formed in our system. This is supported by the comparison with the results of Rabinovitch and colleagues, discussed below.

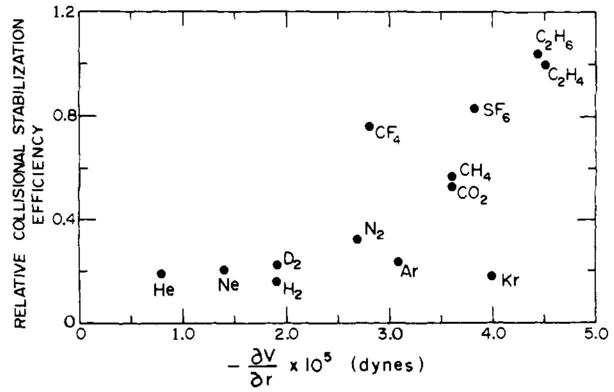

Figure 6. Dependence of relative collisional stabilization efficiencies on $-(\partial V/\partial r)$ (see text).

No definitive reasons can be ascribed to the marked discrepancy between the present study and that of Anicich and Bowers, although there certainly are substantial differences in the type of reaction investigated as well as in the experimental conditions.

2. Neutral Systems. Table III presents a comparison of

Table III. Relative Collisional Stabilization Efficiencies in Ionic and Neutral Systems[a]

M	Relative stabilization efficiency for $(C_5H_9^+)^*$	$(CH_3NC)^*$ [b]	$(C_2H_5NC)^*$ [c]
He	0.19	0.24	0.27
Ne	0.21	0.28	0.30
Ar	0.23_5	0.28	0.39
Kr	0.19	0.24	0.46
H_2	0.16_5	0.24	0.26
D_2	0.22	0.26	
N_2	0.32_5	0.38	0.45
CO	0.33	0.46	
CO_2	0.53	0.55	0.70
SO_2	0.62	0.82	
CH_4	0.57	0.61	<0.70
CD_4	0.58	0.57	
CF_4	0.76	>0.60	
CH_3F	0.57	0.68	
CH_2F_2	0.71	0.66	
SF_6	0.83	0.65	
C_2H_4	(1.00)	0.76	1.00
CH_3NC		(1.00)	
C_2H_5NC			(1.00)
C_2H_6	1.02	0.76	1.00
C_2D_6	0.98	0.69	
C_3H_8		0.79	0.99
C_4H_{10}		1.00	0.95
C_5H_{12}		1.01	0.98
C_6H_{14}		0.99	1.02

[a] For each column numbers are relative to unity for the value given in parentheses. [b] Measured at 281°. [c] Measured at 231°.

our results with the relative stabilization efficiencies obtained by Rabinovitch and colleagues for the deactivation of $(CH_3NC)^*$[13] and $(C_2H_5NC)^*$.[14] It should be noted that the monatomic gases are more efficient stabilizers for $(C_2H_5NC)^*$ than for $(CH_3NC)^*$ when compared to more complex bath gases. This has been attributed,[14] at least in part, to improved matching of moments of inertia and lightening of the angular momentum restrictions in the $(C_2H_5NC)^*$ case, since both systems have nearly the same average excitation energy and threshold energy for decomposition.

The above example illustrates the difficulties of making meaningful quantitative comparisons of data obtained from different systems when a collision complex model is used to interpret the results. Quantitative comparisons of the present data for collisional deactivation of $(C_5H_9^+)^*$ with the neutral system results are made even more difficult by the fact that we know neither the excitation energy nor the critical decomposition energy for the ionic system. In addition, nothing can be said about angular momentum restrictions since the structure of $C_5H_9^+$ is unknown.

Nevertheless we feel that the comparison in Table III provides qualitative evidence that similar deactivation mechanisms are operative in the ionic and neutral systems. The total range in efficiencies is approximately the same and, more importantly, the general trend of increasing efficiency with increasing molecular complexity (until a maximum efficiency is reached) is evident in both the ionic and neutral systems. This leads us to the conclusion that the collisional deactivation of $(C_5H_9^+)^*$ is best described by the collision complex model of Lin and Rabinovitch.[16] In terms of this model, the fact that substitution of D for H in both methane and ethane has practically no effect on the collision efficiencies indicates that very little energy redistribution occurs involving the vibrational modes of the bath gas but that the major energy redistribution process involves the transitional modes of the collision complex.

It can be seen from Table III that monatomic and diatomic collision gases are less efficient stabilizers relative to polyatomic species than they are in the neutral systems. Current and Rabinovitch[17] have shown that inefficient collision gases (such as the rare gases) become even less effective compared to efficient collision gases (complex polyatomic species) as the energy which has to be removed for collisional stabilization increases. This excess energy is approximately 3 kcal mol^{-1} in the isocyanide systems and is unknown, but is probaly larger, for the ionic system. If we assume that $C_5H_7^+$ has the most stable cyclopentenyl structure ($\Delta H_f = 200$ kcal mol^{-1}[45]), the reaction of $C_3H_5^+$ ($\Delta H_f = 226$ kcal mol^{-1}[46]) with ethylene produces $C_5H_9^+$ ions with 39 kcal mol^{-1} excess energy relative to ground state $C_5H_7^+ + H_2$. It is unlikely that this amount of energy must be removed for stabilization of $C_5H_9^+$, suggesting either that the $C_5H_7^+$ product does not have the most stable structure or that the reverse reaction, addition of M_2 to $C_5H_7^+$, has a significant activation energy. It is likely that the excess energy is greater in the ionic system than in the neutral system; however, it is this uncertainty which makes more quantitative discussion of the present results impossible.

Finally, we cannot preclude the possibility that the calculations (section D) resulting in the "best" values for the relative stabilization efficiencies of polar bath gases may have overestimated the collision rate and that polar molecules do have higher efficiencies than their nonpolar counterparts. This could arise if the stronger ion-dipole interactions resulted in a longer lived collision complex in which energy redistribution involving the vibrational modes of the bath gas became more important.

Acknowledgment. P. G. M. would like to thank Professor J. L. Beauchamp for helpful discussions and encouragement during the period when this work first was being contemplated. The authors are indebted to the National Research Council of Canada for financial support and to Professor M. T. Bowers for communication of results prior to publication.

Appendix

The formation of $C_5H_7^+$ and $C_5H_9^+$ type ions by reaction of $C_3H_5^+$ with C_2H_6 or C_2D_6 in ethylene–ethane mixtures has been discussed in the text. From the data of Table II, we have inferred the following reactions as also occurring in these mixtures. With C_2H_6 only the formation of $C_3H_7^+$ is experimentally detectable.

(i) C_2 ions

$$C_2D_6^+ + C_2D_6 \longrightarrow C_2D_4^+ + C_2D_6 + D_2 \qquad \text{(A1)}$$

$$k \sim 1.8 \times 10^{-11}\ \text{cm}^3\ \text{molecule}^{-1}\ \text{sec}^{-1}$$

$$C_2D_6^+ + C_2H_4 \longrightarrow C_2D_4^+ + C_2H_4D_2 \qquad \text{(A2)}$$

$$C_2H_4^+ + C_2D_6 \longrightarrow C_2D_4^+ + C_2H_4D_2 \qquad \text{(A3)}$$

$$k \sim 1.1 \times 10^{-10}\ \text{cm}^3\ \text{molecule}^{-1}\ \text{sec}^{-1}$$[47]

(ii) $C_3(H,D)_5^+$ ions

$$C_2D_4^+ + C_2H_4 \longrightarrow C_3(H,D)_5^+ + C(H,D)_3 \qquad \text{(A4)}$$

(iii) $C_3(H,D)_7^+$ ions

$$C_2H_4^+ + C_2D_6 \longrightarrow C_3(H,D)_7^+ + C(H,D)_3 \qquad \text{(A5)}$$

(iv) $C_4(H,D)_7^+$ ions

$$C_3H_5^+ + C_2D_6 \longrightarrow C_4(H,D)_7^+ + C(H,D)_4 \qquad \text{(A6)}$$

Reaction A1 has previously been studied by Blair, *et al.*,[47] and by Munson, *et al.*[48] Reaction A3 has been observed by Ausloos, *et al.*,[49] who also reported a reaction similar to A2 involving $C_2H_6^+ + C_2D_4$. Finally, the nondeuterated analog of reaction A5 has been studied by Blair, *et al.*,[47] who report a rate constant of $>5 \times 10^{-12}$ cm^3 molecule^{-1} sec^{-1}.

References and Notes

(1) Address correspondence to this author.
(2) C. Zener, *Phys. Rev.*, **37**, 556 (1931).
(3) L. Landau and E. Teller, *Phys. Z. Sowjetunion*, **10**, 34 (1936), cited in ref 5 and 6.
(4) R. N. Schwartz, A. I. Slawsky, and K. F. Herzfeld, *J. Chem. Phys.*, **20**, 1591 (1952).
(5) K. F. Herzfeld and T. A. Litovitz, "Absorption and Dispersion of Ultrasonic Waves," Academic Press, New York, N. Y., 1959.
(6) T. L. Cottrell and J. C. McCoubrey, "Molecular Energy Transfer in Gases," Butterworths, London, 1961.
(7) B. Stevens, *Mol. Phys.*, **3**, 589 (1960).
(8) R. L. Brown and W. Klemperer, *J. Chem. Phys.*, **41**, 3072 (1964).
(9) J. I. Steinfeld and W. Klemperer, *J. Chem. Phys.*, **42**, 3475 (1965).
(10) J. I. Steinfeld, *J. Chem. Phys.*, **44**, 2740 (1966).
(11) P. Borrell, *Advan. Mol. Relaxation Processes*, 1, 69, (1967).
(12) F. J. Fletcher, B. S. Rabinovitch, K. W. Watkins, and D. J. Locker, *J. Phys. Chem.*, **70**, 2823 (1966).
(13) S. C. Chan, B. S. Rabinovitch, J. T. Bryant, L. D. Spicer, T. Fujimoto, Y. N. Lin, and S. P. Pavlou, *J. Phys. Chem.*, **74**, 3160 (1970).
(14) S. P. Pavlou and B. S. Rabinovitch, *J. Phys. Chem.*, **75**, 1366, 2164 3037 (1971).
(15) F. M. Wang, T. Fujimoto, and B. S. Rabinovitch, *J. Phys. Chem.*, **76**, 1935 (1972).
(16) Y. N. Lin and B. S. Rabinovitch, *J. Phys. Chem.*, **74**, 3151 (1970).
(17) J. H. Current and B. S. Rabinovitch, *J. Chem. Phys.*, **40**, 2742 (1964).
(18) G. H. Kohlmaier and B. S. Rabinovitch, *J. Chem. Phys.*, **38**, 1692 (1963).
(19) J. H. Georgakakos an B. S. Rabinovitch, *J. Chem. Phys.*, **56**, 5921 (1972), and references contained therein.
(20) B. S. Rabinovitch, H. F. Carroll, J. D. Rynbrandt, J. H. Georgakakos, B. A. Thrush, and R. Atkinson, *J. Phys. Chem.*, **75**, 3376 (1971).
(21) H. K. Shin, *J. Chem. Phys.*, **42**, 1734 (1965).
(22) G. Gioumousis and D. P. Stevenson, *J. Chem. Phys.*, **29**, 294 (1958).
(23) Qualitative inferences concerning relative collisional deactivation efficiencies can be drawn from the magnitudes of termolecular ion–molecule rates. Recent reviews of many of these results have been presented by Ferguson[24] and by Kebarle.[25]
(24) E. E. Ferguson, "Ion-Molecule Reactions," J. L. Franklin, Ed., Plenum Press, New York, N. Y., 1972, Chapter 8.

(25) P. Kebarle, ref 24, Chapter 7.

(26) P. S. Gill, Y. Inel, and G. G. Meisels, *J. Chem. Phys.*, **54**, 2811 (1971).

(27) V. G. Anicich and M. T. Bowers, *J. Amer. Chem. Soc.*, in press.

(28) J. J. Myher and A. G. Harrison, *Can. J. Chem.*, **46**, 101 (1968).

(29) T. O. Tiernan and J. H. Futrell, *J. Phys. Chem.*, **72**, 3080 (1968).

(30) M. T. Bowers, D. D. Elleman, and J. L. Beauchamp, *J. Phys. Chem.*, **72**, 3599 (1968).

(31) A. A. Herod and A. G. Harrison, *Int. J. Mass Spectrom. Ion Phys.*, **4**, 415 (1970).

(32) A. G. Harrison and A. A. Herod, *Can. J. Chem.*, **48**, 3549 (1970).

(33) In the absence of the collision-induced decomposition of $(C_5H_9^+)^*$ to $C_5H_7^+ + H_2$ the reaction scheme would predict that the ratio $[C_5H_9^+]/[C_5H_7^+]$ should increase linearly with pressure over the entire pressure range. In fact, as has been pointed out,[30] the ratio levels off at about 6.5 in pure ethylene.

(34) S. K. Gupta, E. G. Jones, A. G. Harrison, and J. J. Myher, *Can. J. Chem.*, **45**, 3107 (1967).

(35) F. A. Baker and J. B. Hasted, *Phil. Trans. Roy. Soc. London*, **261**, 33 (1966).

(36) Nonreactive collisions may relax $C_3H_5^+$ to the bottom of the trapping potential well. Thus average ion kinetic energies below those employed by Harrison and Herod (0.53 to 0.21 eV) are possible, and the measured value of k_a should rise accordingly.

(37) S. E. Butrill, *J. Chem. Phys.*, **58**, 656 (1973).

(38) A. S. Blair and A. G. Harrison, *Can. J. Chem.*, **51**, 1645 (1973).

(39) B. H. Solka and A. G. Harrison, paper presented at the 21st Annual Conference on Mass Spectrometry, San Francisco, Calif., May 1973.

(40) We do not intend to imply that, under the present experimental conditions, the reactant ions have 0.3–0.4 eV kinetic energy and that "locking-in" of the dipole occurs. Indeed there is substantial evidence that "locking-in" does not occur.[41-43] Rather we suggest that for secondary or higher order ions the effective kinetic energy is such that this model may be used to estimate the collision rate coefficient. It is distinctly possible that the collision process(es) resulting in the formation of these ions (as well as other nonreactive collisions) may relax the ions to the bottom of the trapping potential well and that they thus have substantially lower kinetic energies than the 0.3–0.4 eV which primary ions possess.[31,44]

(41) J. V. Dugan and J. L. Magee, NASA Report TN-D-3229, Feb 1966.

(42) J. V. Dugan and J. L. Magee, *J. Chem. Phys.*, **47**, 3103 (1967).

(43) J. V. Dugan and R. B. Canwright, *J. Chem. Phys.*, **56**, 3623 (1972).

(44) A. A. Herod, A. G. Harrison, and N. A. McAskill, *Can. J. Chem.*, **49**, 2217 (1971).

(45) F. P. Lossing, paper presented at the 22nd Annual Conference on Mass Spectrometry, Philadelphia, Pa., May, 1974.

(46) F. P. Lossing, *Can. J. Chem.*, **49**, 357 (1971).

(47) A. S. Blair, E. J. Heslin, and A. G. Harrison, *J. Amer. Chem. Soc.*, **94**, 2935 (1972).

(48) M. S. B. Munson, J. L. Franklin, and F. H. Field, *J. Phys. Chem.*, **68**, 3098 (1964).

(49) P. Ausloos, R. E. Rebbert, and L. W. Sieck, *J. Chem. Phys.*, **54**, 2612 (1971).

Carbon-13 Nuclear Magnetic Resonance Studies of Organometallic Compounds. VII. 1,5-Cyclooctadieneplatinum(II) Derivatives[1]

Malcolm H. Chisholm, Howard C. Clark,* Leo E. Manzer, J. B. Stothers,[2] and John E. H. Ward

Contribution from the Department of Chemistry, The University of Western Ontario, London, Ontario N6A 3K7, Canada.

Received June 5, 1974

Abstract: The ^{13}C nmr spectra have been obtained for three series of π-bonded 1,5-cyclooctadieneplatinum(II) derivatives of the type $[CODPt(CH_3)R]$, $[CODPt(CH_3)L]^+PF_6^-$, and $[CODPtRR']$, where R and R′ are anionic substituents and L is a neutral donor. The ^{13}C shieldings and $^{13}C-^{195}Pt$ coupling constants are discussed and compared with ^{13}C nmr parameters derived from related platinum(II) complexes containing σ-bonded carbons. The ^{13}C shielding and coupling constant trends of the π-bonded carbons are generally found to parallel those trends for the σ-bonded carbons.

^{13}C nuclear magnetic resonance investigations[3-20] of π-bonded olefin transition metal complexes are now commonplace. However, there have been only a few reports[3,4,6,16,17] which involve a detailed examination of series of closely related compounds for which both the olefinic carbon shieldings *and* metal–olefinic carbon coupling constants have been recorded.

We now wish to report a *systematic* study of three series of π-bonded 1,5-cyclooctadiene[21] complexes of platinum(II) (^{195}Pt, 34% natural abundance, $I = \frac{1}{2}$): $[CODPt(CH_3)R]$ (I), $[CODPt(CH_3)L]^+PF_6^-$ (II), and $[CODPtRR']$ (III), where R and R′ are anionic substituents and L is a neutral donor ligand. For these derivatives, both the olefinic carbon shieldings and $^{13}C-^{195}Pt$ coupling constants of the COD ligand provide useful information about the mode of olefin–metal bonding.

We have specifically selected the chelating ligand COD to eliminate the possibility of rotation about the metal–olefin bond axis, a feature which has been ignored in the majority of previous studies. The cationic complexes, II, were prepared to enable direct comparisons with the ^{13}C nmr parameters derived from analogous σ-bonded platinum(II) complexes of the sort $[DIARSPt(CH_3)L]^+PF_6^-$ [22,23] (A), where L is a neutral ligand. For both series II and A, we have intentionally chosen a variety of L donors whose nmr trans influences[24-26] span a wide range.

Experimental Section

All complexes were prepared as previously described.[27,28] The ^{13}C nmr spectra were measured on a Varian XL-100-15 spectrometer operating in the Fourier transform mode at 25.2 MHz. All spectra were determined with noise-modulated proton decoupling. To identify carbon types, off-resonance decoupled spectra were obtained by offsetting the decoupling single frequency using an offset of 1 kHz. By offsetting the noise-modulated frequency by *ca.* 30 kHz from the optimum value, normal $^1J_{CH}$ values were obtained from the resulting coupled spectra. The spectra were taken on chloroform-*d*, methylene chloride-d_2, and acetone-d_6 solutions in 5-mm sample tubes and were calibrated using the solvent resonances as secondary standards.[29]

Results

The shieldings and coupling constants obtained from the ^{13}C nmr spectra of the complexes of series I–III are assembled in Tables I–III. The ^1H nmr parameters for **1–13** have already been reported.[27,28] No relative sign determinations for the coupling constants were made.

For complexes **1–7**, the high field resonances of their ^{13}C nmr spectra were assigned on the basis of their relative in-

Clark, et al. / 1,5-Cyclooctadieneplatinum(II) Derivatives